ON THE CALCULATION OF HEAD IMPACT MOTION USING EXPERIMENTAL DATA

by

G. Gustafsson and L. Karlsson

Department of Mechanical Engineering, University of Luleå, Luleå, Sweden

ABSTRACT

Numerous head impact tests have been carried out by the Biomechanics department of the Highway Safety Research Institute, University of Michigan, Ann Arbor, during the past few years. The purpose of this work is to investigate the head motion during impact loading (the unloading phase is not considered) and especially to determine if the head slips on the impactor or rotates around it. Data from three different types of tests have been analysed: Front, side and rear impacts on human heads. The data consists of linear and angular accelerations and velocities for the head (considered as a rigid body). These four quantities are some of the most common that have been suggested as primary causes of injury. By using experimental data the position of the instantaneous point of rotation was determined as a function of time during impact loading. It was found that slip occurs between the impactor and the head with very few exceptions. It was also found that the human skull performs plane motion after front or rear impact. This is probably due to the symmetry around the midsagittal plane. In side impact on the human skull it was found that the motion is three-dimensional.

INTRODUCTION

During the past few years numerous head impact tests on human cadavers have been carried out by the Biomechanics department of the Highway Safety Research Institute, University of Michigan, Ann Arbor. The purpose of this paper is to investigate the motion of the head during impact loading (the unloading phase is not considered here), and especially to determine whether or not slip occurs between the head and the impactor. Data from three different types of tests is analysed: Front, side and rear impacts on human heads. The data consists of linear and angular accelerations and velocities for the head (considered as a rigid body). The linear and angular accelerations are some of the most common quantities that have been suggested as primary causes of injury.

EXPERIMENTS

A complete description of the testing procedure which gives the desired data of head motion due to impact is given in [1]. However, the testing procedure will be briefly outlined here. The head motion is determined by using nine accelerometers which give a redundant system of nine equations. The solution for the six components of acceleration is obtained by using the method of least squares. The data are then transformed to a laboratory reference frame $(\hat{I},\hat{J},\hat{K})$, figure 1. This frame is also used for the determination of the distance between the anatomical center (see definition below) and the instantaneous point of rotation. The Frenet-Serret frame is defined in figure 1, where S(t) is the distance travelled along the curve as a function of time t. κ is the curvature at the point P, see [2]. The anatomical frame is shown in figure 2.

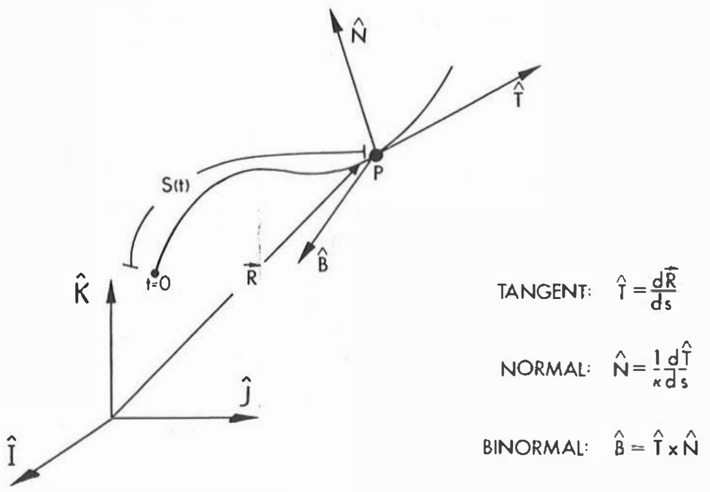

Figure 1. Laboratory reference frame $(\hat{I},\hat{J},\hat{K})$ and Frenet-Serret frame $(\hat{T},\hat{N},\hat{B})$.

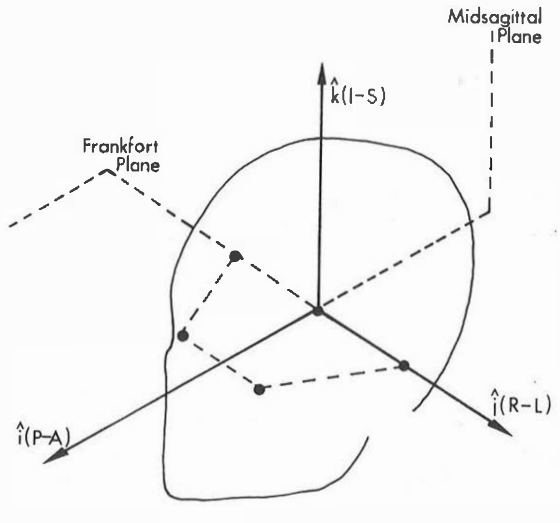

Figure 2. Anatomical frame $(\hat{i},\hat{j},\hat{k})$.

The anatomical i-axis is defined along the intersection of the Frankfort and midsagittal planes (see figure 2) in the posterior-to-anterior (P-A) direction. The j-axis is defined along the line joining the two superior edges of the auditory meati, in the right-to-left (R-L) direction. This j-axis, which lies in the Frankfort plane, is perpendicular to the midsagittal plane at the anatomical center, which is taken as the origin of the anatomical frame. Finally, the k-axis is defined as the cross-product of the unit vectors $\bar{i}$ and

$\hat{j}$. Thus, it will be located in the midsagittal plane in the interior-to-superior (I-S) direction. The anatomical center is located in the middle of the line between the ears in the Frankfort plane.

MATHEMATICAL MODEL

In order to assess whether or not slip between the head and the impactor occurs, the instantaneous point of rotation is determined. This point is determined as the point which at a certain instant of time has the minimum acceleration in the $\hat{N}$-direction. Its location is then compared with the location of the impact point found from radiographs of the head, [1]. If these two points coincide, then the head does not slip on the impactor.

The velocity of a point in space is

$$\vec{V}_p = v\hat{T} \tag{1}$$

The acceleration then becomes

$$\vec{A}_p = \frac{d\vec{V}_p}{dt} = \frac{dv}{dt}\hat{T}+\kappa v^2\hat{N} \tag{2}$$

The component in the $\hat{N}$-direction is

$$\vec{A}_p\cdot\hat{N} = \frac{|\vec{V}_p x\vec{A}_p|}{|\vec{V}_p|} = \kappa v^2 \tag{3}$$

The velocity of a point in the laboratory reference system is

$$\vec{V}_p = \vec{V}+\vec{\omega}x\vec{r} \tag{4}$$

where $\vec{V}$ is the linear velocity of the anatomical center, figure 2, $\vec{\omega}$ is the angular velocity and $\vec{r}$ the vector from the anatomical center to an arbitrary point. The acceleration then becomes

$$\vec{A}_p = \frac{d\vec{V}_p}{dt} = \vec{A}+\dot{\vec{\omega}}x\vec{r}+\vec{\omega}x\dot{\vec{r}} \tag{5}$$

where $\vec{A}$ is the linear acceleration of the anatomical center, $\dot{\vec{\omega}}$ is the angular acceleration and $\dot{\vec{r}}$ is the derivative of $\vec{r}$ with respect to time. The time of impact loading is a few milliseconds which is the time interval studied here. In this time interval $|\vec{\omega}||\dot{\vec{r}}|$ is small as compared to $|\vec{A}|$ and $|\dot{\vec{\omega}}||\vec{r}|$. Therefore the last term in (5) can be neglected. The cross-product in (3) is then obtained as

$$\vec{V}_p x\vec{A}_p = \vec{V}x\vec{A}+(\vec{V}\cdot r)\dot{\vec{\omega}}-(\vec{A}\cdot\vec{r})\vec{\omega}+((\vec{A}\cdot\vec{\omega})-(\vec{V}\cdot\dot{\vec{\omega}}))\vec{r}+(\vec{r}\cdot(\dot{\vec{\omega}}x\vec{\omega}))\vec{r} \tag{6}$$

The last term in (6) is very small as compared to the other terms because $\vec{\omega}$ and $\dot{\vec{\omega}}$ are almost parallel. Thus, one obtains

$$\vec{V}_p x \vec{A}_p = (V_y A_z - V_z A_y + (A_y \omega_y + A_z \omega_z - V_y \dot{\omega}_y - V_z \dot{\omega}_z) r_x +$$
$$+ (V_y \dot{\omega}_x - A_y \omega_x) r_y + (V_z \dot{\omega}_x - A_z \omega_x) r_z) \hat{I} +$$
$$+ (V_z A_x - V_x A_z + (V_x \dot{\omega}_y - A_x \omega_y) r_x + (A_x \omega_x + A_z \omega_z - V_x \dot{\omega}_x - V_z \dot{\omega}_z) r_y +$$
$$+ (V_z \dot{\omega}_y - A_z \omega_y) r_z) \hat{J} + (V_x A_y - V_y A_x + (V_x \dot{\omega}_z - A_x \omega_z) r_x +$$
$$+ (V_y \dot{\omega}_z - A_y \omega_z) r_y + (A_x \omega_x + A_y \omega_y - V_x \dot{\omega}_x - V_y \dot{\omega}_y) r_z) \hat{K} \qquad (7)$$

The velocity is

$$\vec{V}_p = (V_x - \omega_z r_y + \omega_y r_z) \hat{I} + (V_y + \omega_z r_x - \omega_x r_z) \hat{J} + (V_z - \omega_y r_x + \omega_x r_y) \hat{K} \qquad (8)$$

Now the acceleration in the $\hat{N}$-direction can be written as

$$\vec{A}_p \cdot \hat{N} = \sqrt{\frac{Ar^2 + Br + C}{Dr^2 + Er + F}} \qquad (9)$$

where $r = |\vec{r}|$. Minimization of $\vec{A}_p \cdot \hat{N} = |\vec{V}_p x \vec{A}_p| / |\vec{V}_p|$ with respect to r for fixed angles gives

$$r_{1,2} = \frac{CD-AF}{AE-BD} \pm \sqrt{\left(\frac{CD-AF}{AE-BD}\right)^2 + \frac{CE-BF}{AE-BD}} \qquad (10)$$

The acceleration is determined for the two roots and the root giving the lowest acceleration is the distance between the anatomical center and the instantaneous point of rotation. The factors A,B,C,D,E and F are then determined for the three different cases front impact, side impact and rear impact. The expressions for the factors A,B,C,D,E and F will be shown only for the case of front impact.

In the case of front impact the instantaneous point of rotation is searched only in the midsagittal plane, i.e. the components of $\vec{r}$ are approximately

$$r_x = r\cos\theta \quad r_y = 0 \quad r_z = r\sin\theta \qquad (11a,b,c)$$

The angle θ is defined in figure 3. The subscripts x, y and z denote components in the I-, J- and K-directions, respectively. The change of the components of $\vec{r}$ from the anatomical frame $(\hat{i},\hat{j},\hat{k})$ to the laboratory frame $(\hat{I},\hat{J},\hat{K})$ is neglected since the time interval for the loading phase is very short (only a few ms). The reason for searching only in the midsagittal plane is the symmetry of the head with respect to this plane.

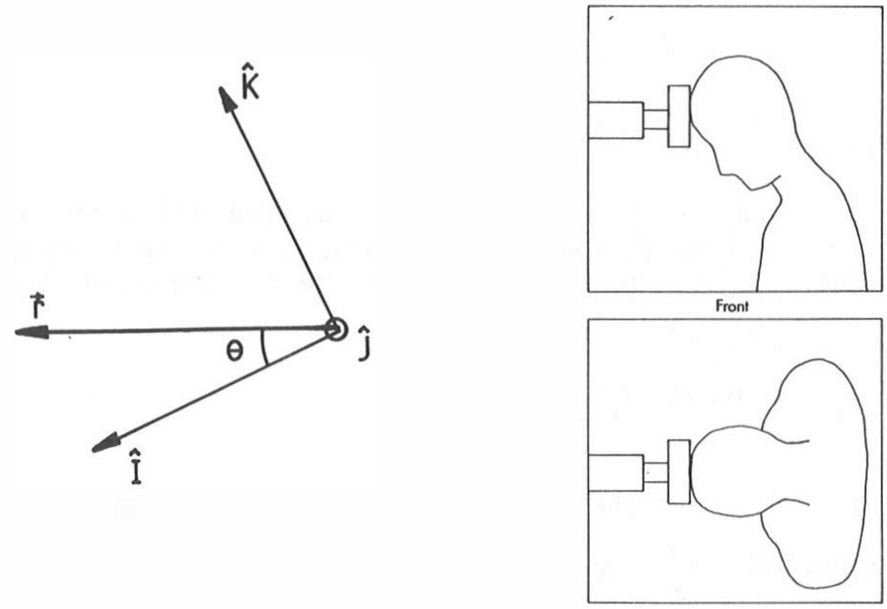

Figure 3. Front impact. $(\hat{i},\hat{j},\hat{k})$ and $(\hat{I},\hat{J},\hat{K})$ coincide before impact.

The anatomical frame $(\hat{i},\hat{j},\hat{k})$, figure 2, coincides with the laboratory reference frame $(\hat{I},\hat{J},\hat{K})$ before impact. The factors A,B,C,D,E and F are obtained as

$$A = ((V_x\dot{\omega}_y-A_x\omega_y)\cos\theta+(V_z\dot{\omega}_y-A_z\omega_y)\sin\theta)^2+$$
$$((A_y\omega_y+A_z\omega_z-V_y\dot{\omega}_y-V_z\dot{\omega}_z)\cos\theta+(V_z\dot{\omega}_x-A_z\omega_x)\sin\theta)^2+$$
$$((V_x\dot{\omega}_z-A_x\omega_z)\cos\theta+(A_x\omega_x+A_y\omega_y-V_x\dot{\omega}_x-V_y\dot{\omega}_y)\sin\theta)^2 \tag{12a}$$

$$B = 2(((A_y\omega_y+A_z\omega_z-V_y\dot{\omega}_y-V_z\dot{\omega}_z)\cos\theta+(V_z\dot{\omega}_x-A_z\omega_x)\sin\theta)$$
$$(V_yA_z-V_zA_y)+((V_x\dot{\omega}_y-A_x\omega_y)\cos\theta+(V_z\dot{\omega}_y-A_z\omega_y)\sin\theta)$$
$$(V_zA_x-V_xA_z)+((V_x\dot{\omega}_z-A_x\omega_z)\cos\theta+(A_x\omega_x+A_y\omega_y-V_x\dot{\omega}_x-V_y\dot{\omega}_y)$$
$$\sin\theta)(V_xA_y-V_yA_x)) \tag{12b}$$

$$C = (V_yA_z-V_zA_y)^2+(V_zA_x-V_xA_z)^2+(V_xA_y-V_yA_x)^2 \tag{12c}$$

$$D = \omega_y^{\,2}+(\omega_z\cos\theta-\omega_x\sin\theta)^2 \tag{12d}$$

$$E = 2((V_y\omega_z-V_z\omega_y)\cos\theta+(V_x\omega_y-V_y\omega_x)\sin\theta) \tag{12e}$$

$$F = V_x^{\,2}+V_y^{\,2}+V_z^{\,2} \tag{12f}$$

Here

$$\vec{V} = (V_x, V_y, V_z) \qquad \vec{A} = (A_x, A_y, A_z) \tag{13a,b}$$

$$\vec{\omega} = (\omega_x, \omega_y, \omega_z) \qquad \dot{\vec{\omega}} = (\dot{\omega}_x, \dot{\omega}_y, \dot{\omega}_z) \tag{13c,d}$$

The component of $\vec{V}_p x \vec{A}_p$ in the $\hat{J}$-direction in equation (7) gives the value of r for purely two-dimensional motion. The smallest possible value of this component of the acceleration in the $\hat{N}$-direction is zero which gives

$$r = \frac{V_x A_z - V_z A_x}{(V_x \dot{\omega}_y - A_x \omega_y)\cos\theta + (V_z \dot{\omega}_y - A_z \omega_y)\sin\theta} \tag{14}$$

In the case of side impact the components of the vector $\vec{r}$ are

$$r_x = r\sin\gamma\sin\alpha \qquad r_y = r\cos\gamma \qquad r_z = r\sin\gamma\cos\alpha \tag{15a,b,c}$$

The angles α and γ are defined in figure 4. Now the factors A,B,C,D,E and F in equation (10) can be obtained from equations (7) and (15).

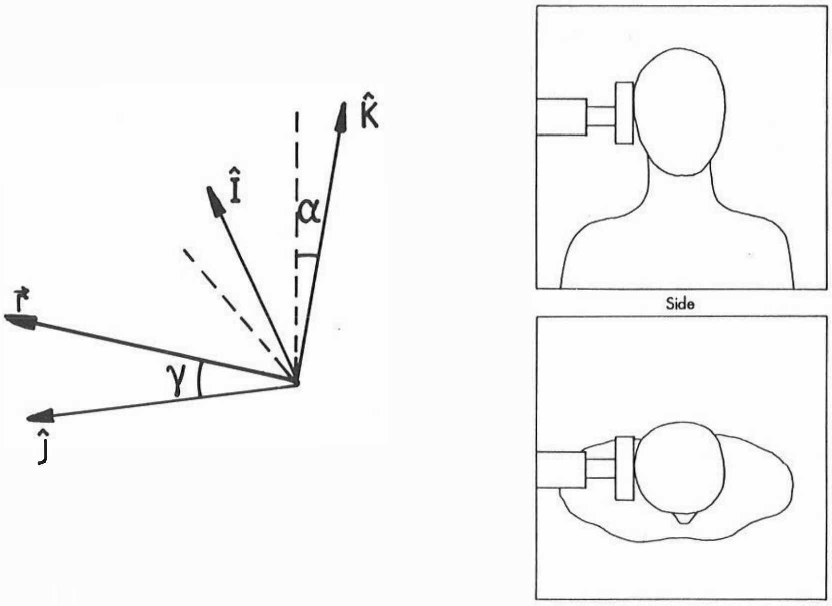

Figure 4. Side impact. $(\hat{i},\hat{j},\hat{k})$ and $(\hat{I},\hat{J},\hat{K})$ coincide before impact.

In the case of rear impact the instantaneous point of rotation is, as in the case of front impact, searched only in the midsagittal plane. The components of the vector $\vec{r}$ then become

$$r_x = -r\cos\theta \qquad r_y = 0 \qquad r_z = r\sin\theta \tag{16a,b,c}$$

The angle θ is defined in figure 5. The factors A,B,C,D,E and F can now be determined from equations (7) and (16).

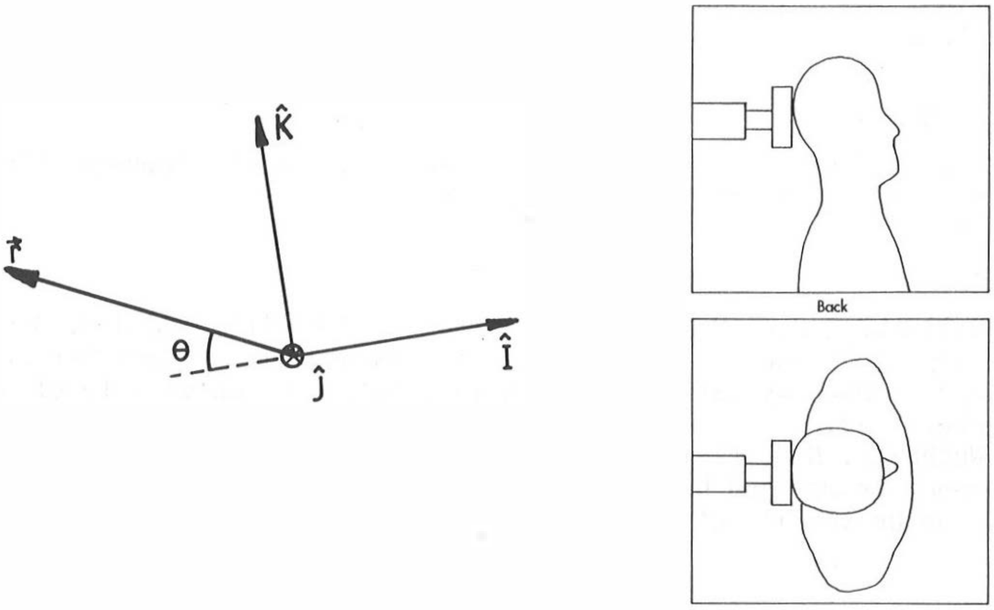

Figure 5. Rear impact.($\hat{i},\hat{j},\hat{k}$) and ($\hat{I},\hat{J},\hat{K}$) coincide before impact.

The angle θ, figures 3 and 5, and the angles α and γ, figure 4, are chosen so that a vector $\vec{r}$, figures 3, 4, and 5,from the anatomical center passes through the point of impact. An alteration of $\pm 10^0$ of the angles θ, α and γ from the chosen values varies the calculated distance r(t) only a few percent. If the evaluated value of the distance r agrees with the measured (from radiographs) distance from the anatomical center to the point of impact and this value also does not vary in time, then the head does not slip on the impactor.

RESULTS

Data from five front impact tests, three side impact tests and four rear impact tests are analysed. The distance r in a front impact is shown in figure 6 as a function of time. Here the measured (from radiograph) distance between the point of impact and the anatomical center is 120 mm. The data used in equations (10), (12) and (14) are shown in table 1. Here $\theta=40^0$. The evaluated distance r as a function of time is shown in figure 7 for a side impact test, and in figure 8 for a rear impact test. The measured distance between the point of impact and the anatomical center is for the side impact 60 mm and it is 100 mm for the rear impact. In side impact $\gamma=0^0$ and $\alpha=10^0$ and in rear impact $\theta=40^0$.

CONCLUSIONS

As can be seen from figures 6, 7 and 8 slip does occur in all three types of tests. Slip was questionable only in two cases out of twelwe.

Figures 6 and 8 show that the equation for three-dimensional motion and the equation for two-dimensional motion agree in front impact and in rear impact. In the case of side impact, figure 7, there is disagreement between the equations for two- and three-dimensional motion. In exceptional cases of front and rear impact it was observed that the head motion deviated from two-dimensional motion. This was due to lack of symmetry with respect to the mid-sagittal plane.

ACKNOWLEDGEMENT

We would like to express our gratitude to Mr G. Nusholtz, Highway Safety Research Institute, for helpful discussions.

REFERENCES

1. R.L. Stalnaker, J.W. Melvin, G.S. Nusholtz, N.M. Alem and J.B. Benson. "Head Impact Response". Presented at the Twenty-First Stapp Car Crash Conference. Highway Safety Research Institute, The University of Michigan, September 1977.
2. G.S. Nusholtz, N.M. Alem, J.W. Melvin and R.L. Stalnaker. "Reference frames and head impact motion". Highway Safety Research Institute, The University of Michigan.

Table 1

Evaluated values in the laboratory reference frame $(\hat{I},\hat{J},\hat{K})$ from experimental data. The time step between each value is 0.33 ms starting with the first at 3.33 ms before the peak of the impact force.

$V_x[\frac{m}{s}]$	-0.774, -0.988, -1.23, -1.49, -1.78, -2.08, -2.42, -2.81, -3.26, -3.79
$V_r[\frac{m}{s}]$	-0.037, -0.050, -0.066, -0.090, -0.122, -0.159, -0.192, -0.220, -0.248, -0.283
$V_z[\frac{m}{s}]$	-0.162, -0.237, -0.323, -0.422, -0.533, -0.655, -0.788, -0.940, -1.12, -1.32
$A_x[\frac{m}{s^2}]$	-652., -725., -810., -884., -942., -1010., -1150., -1350., -1590., -1740.
$A_y[\frac{m}{s^2}]$	-45.1, -43.2, -61.5, -91.6, -114., -114., -98.5, -86.9, -97.0, -124.
$A_z[\frac{m}{s^2}]$	-229., -256., -296., -338., -373., -406., -452., -527., -617., -679.
$\omega_x[\frac{1}{s}]$	-0.202, -0.221, -0.254, -0.348, -0.510, -0.690, -0.826, -0.901, -0.961, -1.07
$\omega_r[\frac{1}{s}]$	4.46, 5.54, 6.65, 7.81, 8.95, 9.97, 10.8, 11.6, 12.4, 13.3
$\omega_z[\frac{1}{s}]$	0.001, -0.101, -0.213, -0.336, -0.470, -0.602, -0.708, -0.771, -0.786, -0.777
$\dot{\omega}_x[\frac{1}{s^2}]$	-100., -52.4, -188., -423., -579., -530., -332., -184., -249., -469.
$\dot{\omega}_y[\frac{1}{s^2}]$	3440., 3480., 3660., 3740., 3500., 3000., 2560., 2490., 2740., 2830.
$\dot{\omega}_z[\frac{1}{s^2}]$	-312., -342., -376., -416., -435., -393., -277., -120., 5.61, 29.4

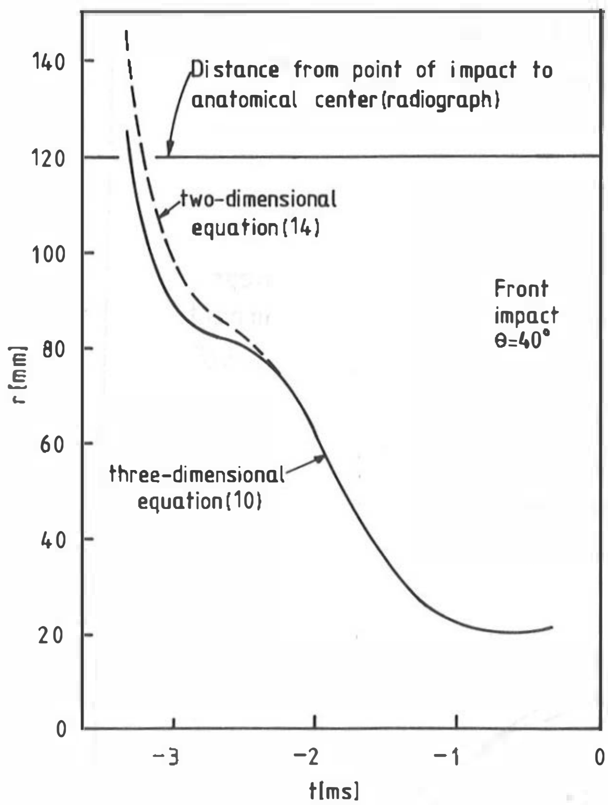

Figure 6. Calculated distance r(t) in a front impact test.

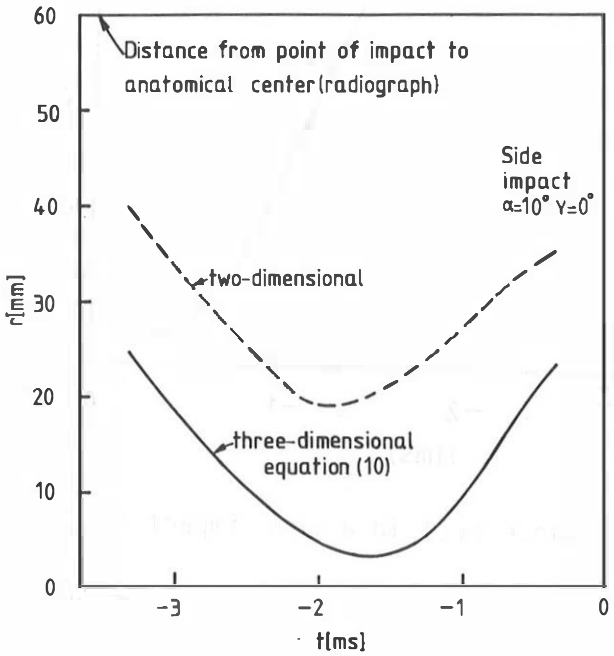

Figure 7. Calculated distance r(t) in a side impact test.

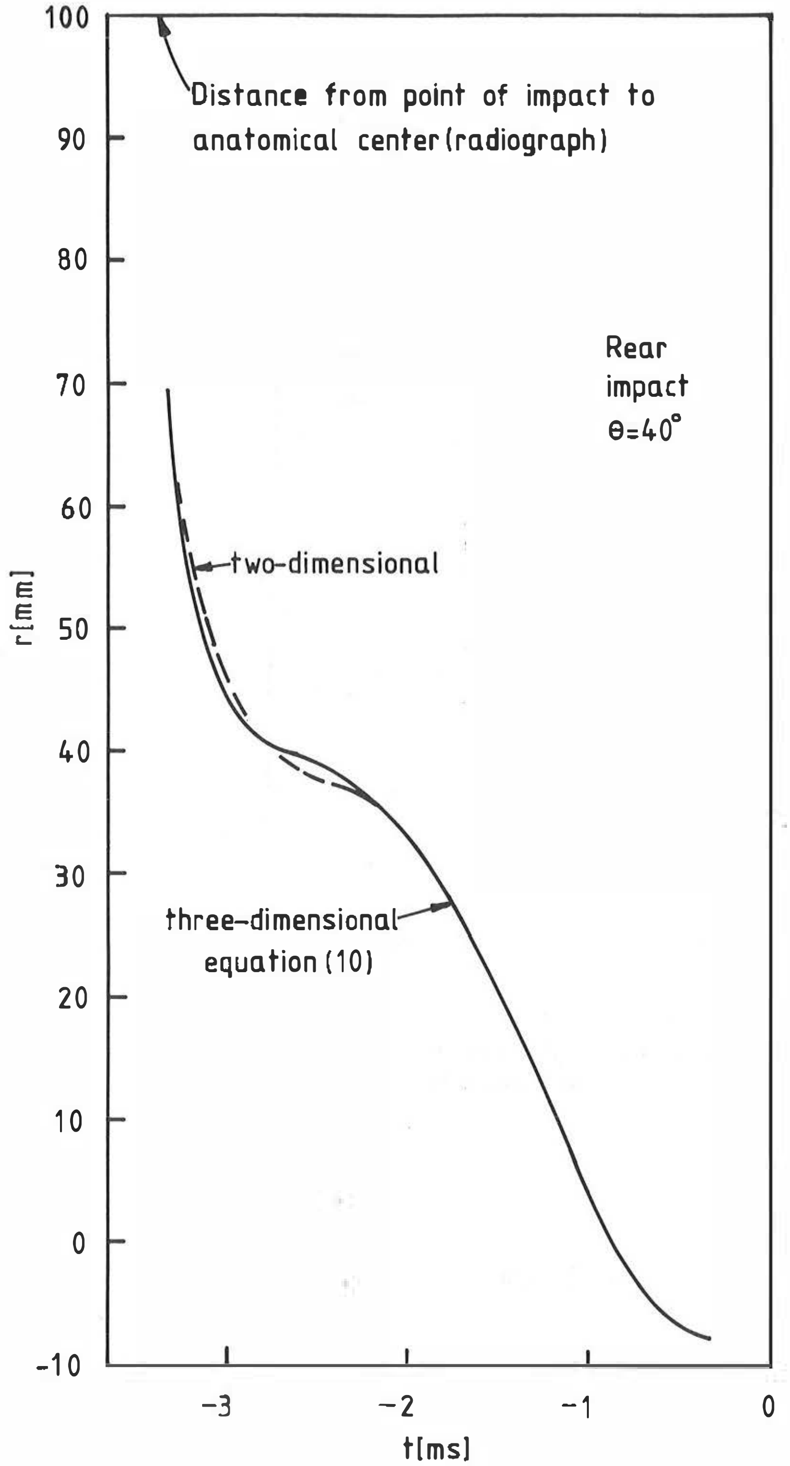

Figure 8. Calculated distance r(t) in a rear impact test.